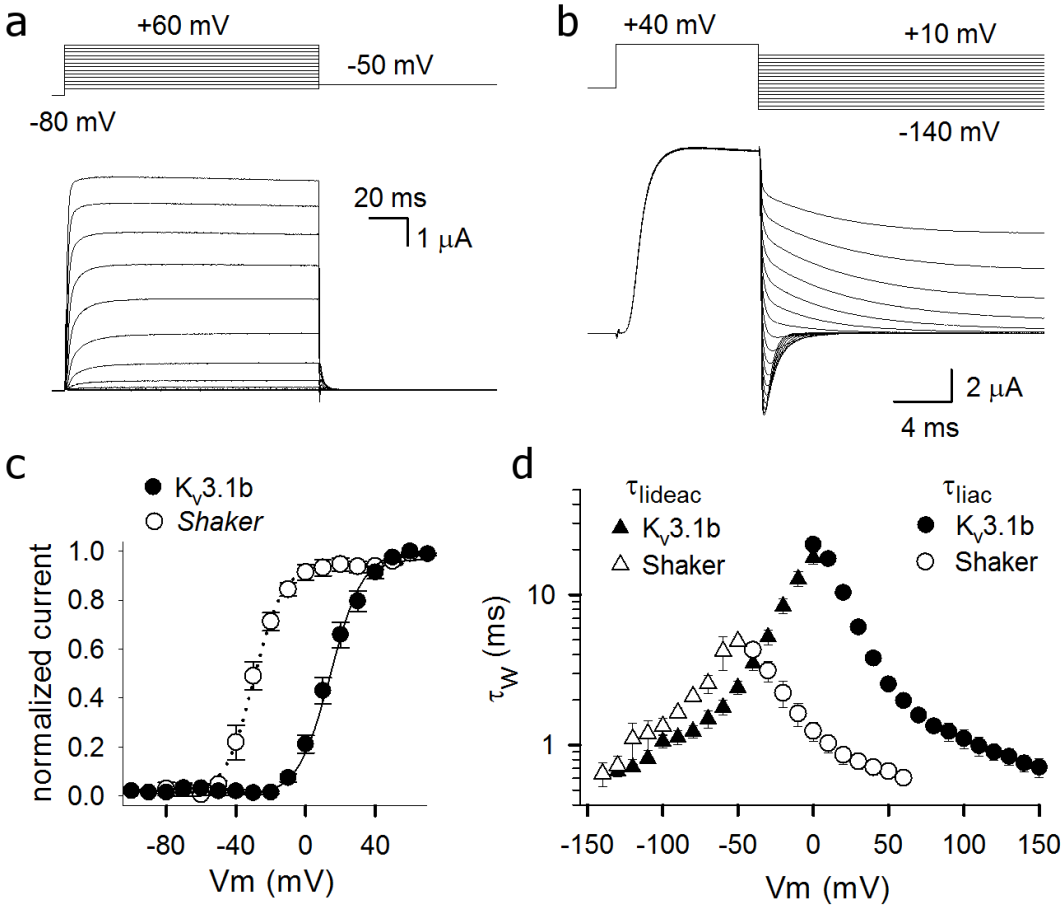

Supplementary Figure 1: K_v3.1b ionic current recordings monitor gate opening and closing.

(**a**) Activating ionic currents (Ii_{ac}) from K_v3.1b obtained using the pulse protocol shown on top. (**b**) Deactivating ionic currents (Ii_{deac}) upon a short +40 mV depolarizing pulse to open the channels. (**c**) Voltage dependence of channel gate opening: conduction (G) versus voltage (GV) curves for K_v3.1b (black circles, *n* = 11) and Shaker (open circles, n = 7) channels determined from the tail currents obtained with pulse protocols shown in **a**. Tail current amplitudes were normalized and plotted as a function of the pulse depolarization potential and the represented GV curves are the average fit to a 2-state Boltzmann equation. Note the high threshold for channel opening in K_v3.1b compared to Shaker. (**d**) Weighted time constants (τ_W) ± SEM of channel gate opening (circles, τ_{liac}) and closing (triangles, τ_{lideac}) for K_v3.1b (black symbol, *n* = 11) and Shaker (open symbols, *n* = 7). These values were obtained from fitting Ii_{ac} and Ii_{deac} with a single and double exponential respectively. Note that K_v3.1b and Shaker displayed similarly fast τ_{liac} and τ_{lideac} kinetics.

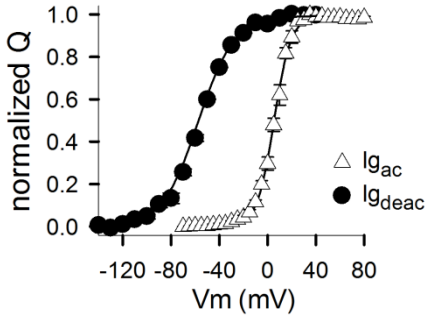

Supplementary Figure 2: Voltage dependence of K_v3.1b VSD deactivation suggests a slow Ig_{deac} component.

The deactivating QV curve (black circles), to determine the voltage dependence of VSD deactivation, was obtained from integrating the Ig_{deac} currents from deactivation pulse protocols shown in Supplementary Fig. 1b. Compared to the voltage dependence of VSD activation (open triangles, which is redisplayed from Supplementary Fig. 1c), the deactivating QV curve located at more negative potentials, displaying a midpoint at -55.5 ± 2.3 mV (n = 6). A similar displacement in the deactivating QV curve was also observed in K_v3.2 channels[1]. The voltage range over which the QV curve was shifted when obtained from a deactivation protocol versus an activation protocol corresponded with the voltage window where τ_{lideac} was slower than τ_{Igdeac} (Supplementary Fig. 1d). As this displacement in voltage dependence of charge movement was not reflected at the ionic current level and K_v3.1b channels close completely at repolarizations stronger than -10 mV, this displacement of the QV curve is most likely due to the presence of a slow, undetectable Ig_{deac} component.

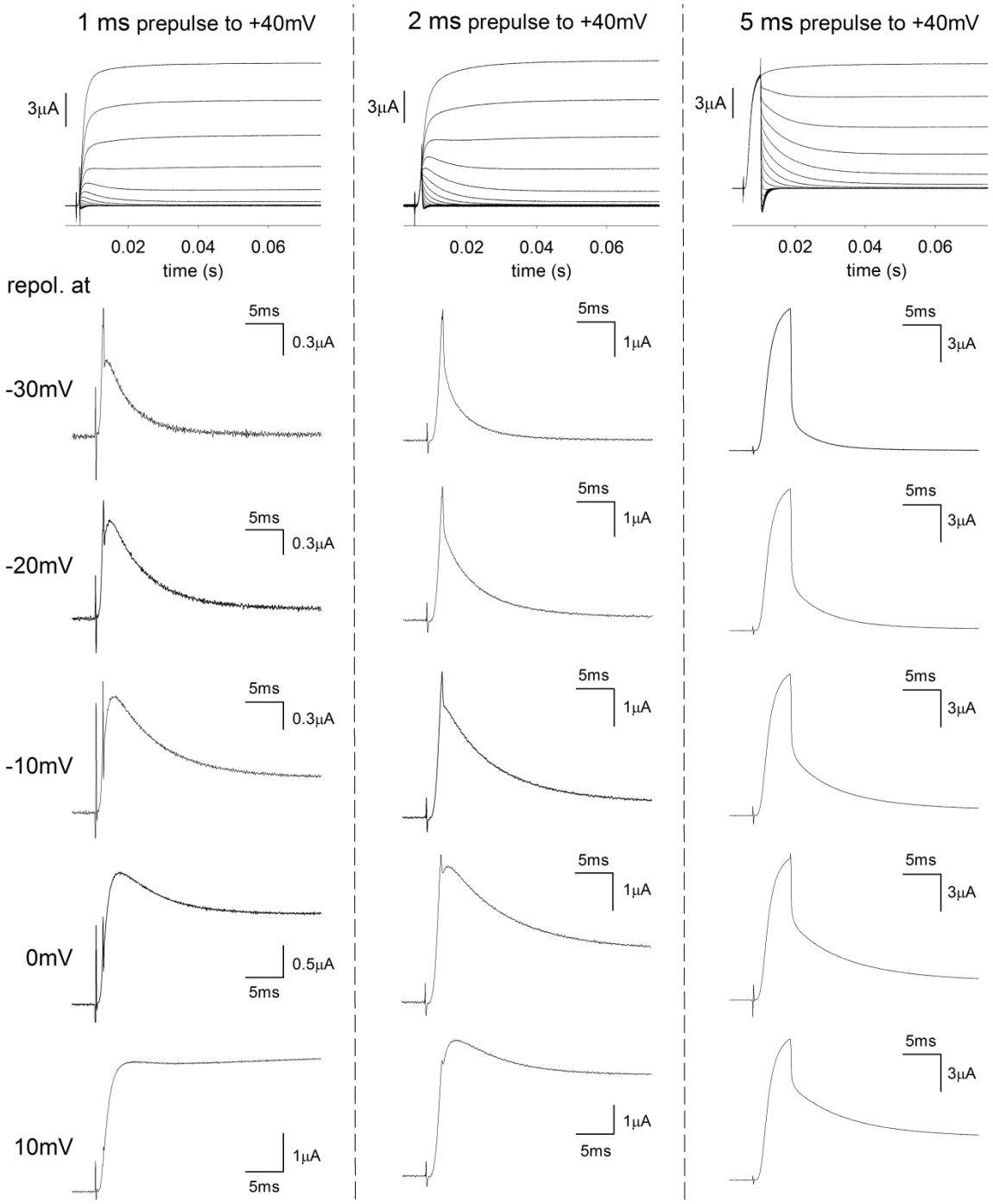

Supplementary Figure 3: K_v3.1b resurgent current is temporally and energetically defined.
Detailed examination of the K_v3.1b ionic currents obtained upon 1 ms (left column), 2 ms (middle column), and 5 ms (right column) depolarizations to +40 mV, followed by repolarizations ranging from -30 mV (top) to 10 mV (bottom). Resurgent current is clearly seen following the 1 ms prepulse between -30 mV and 0 mV, and is completely absent by extending the depolarizing prepulse duration to 5 ms, suggesting that it occurs specifically in response to brief action potential-like pulses to generate a resurgent current at intermediate voltages to complete repolarization of the membrane.

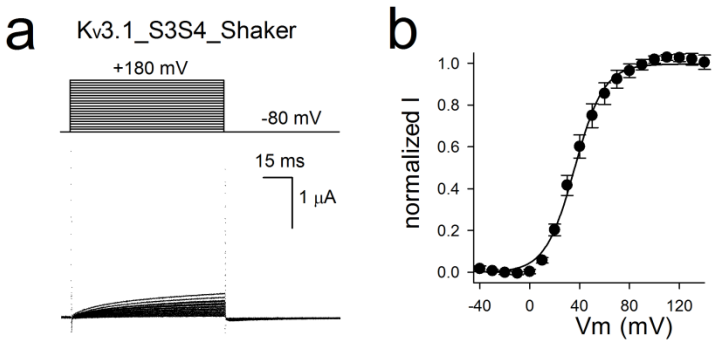

Supplementary Figure 4: Shaker_S3S4_K_v3.1 chimera´s voltage dependence of channel opening.
(**a**) A representative current recording (pulse protocol at top) of the K_v3.1_S3S4_Shaker chimera in 2 mM external and 115 mM internal potassium solution. No currents were found that could be discriminated from leak currents of the oocyte. (**b**) GV curve of Shaker_S3S4_K_v3.1 chimera (*n* = 6) determined from the tail currents obtained with activation pulse protocols (Fig. 6b). Tail current amplitudes were normalized and plotted as a function of the pulse depolarization potential and the represented GV curves are the average fit to a 2-state Boltzmann equation.

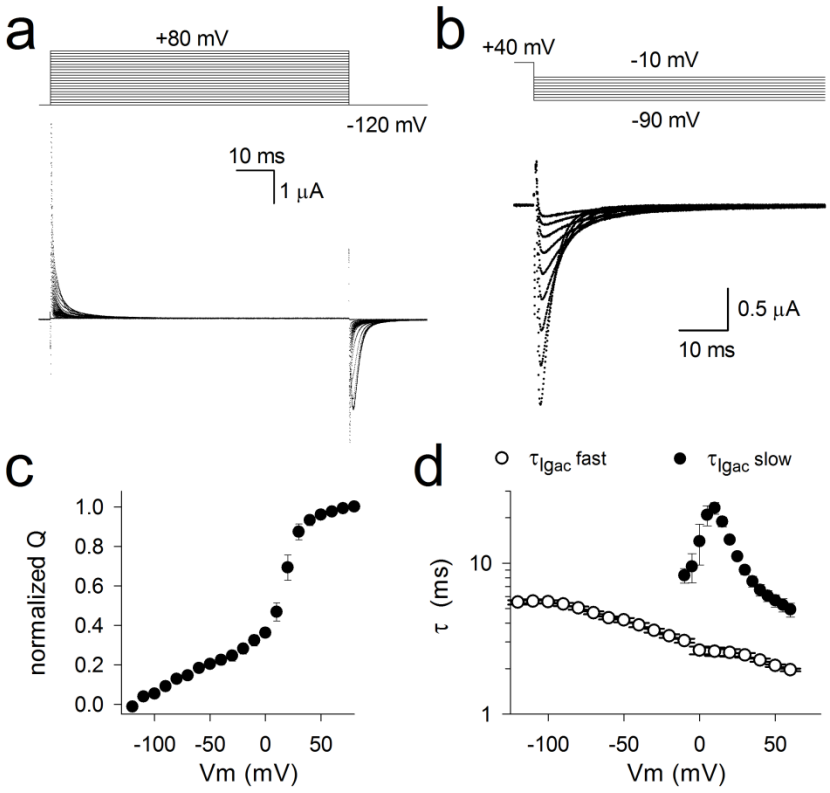

Supplementary Figure 5: Gating currents of the Shaker_S3S4_K_v3.1 W434F chimera.
(**a**) Activation ionic currents of the Sh_S3S4_K_v3.1 W434F chimera from -120 mV to +80 mV in 10 mV steps. (**b**) Deactivation ionic currents of the chimera held at +40 mV and pulsed at 10 mV intervals from -10 mV to -90 mV. (**c**) Q-V curve of the chimera (*n* = 4). (**d**) Time constants of I_{Gac} ± SEM (*n* = 4) plotted versus voltage of the activating pulse. There were two noticeable gating charge components, a fast component that started to move before 0 mV, and a slow component that is responsible for pore opening and emerged with activating pulses above 0 mV.

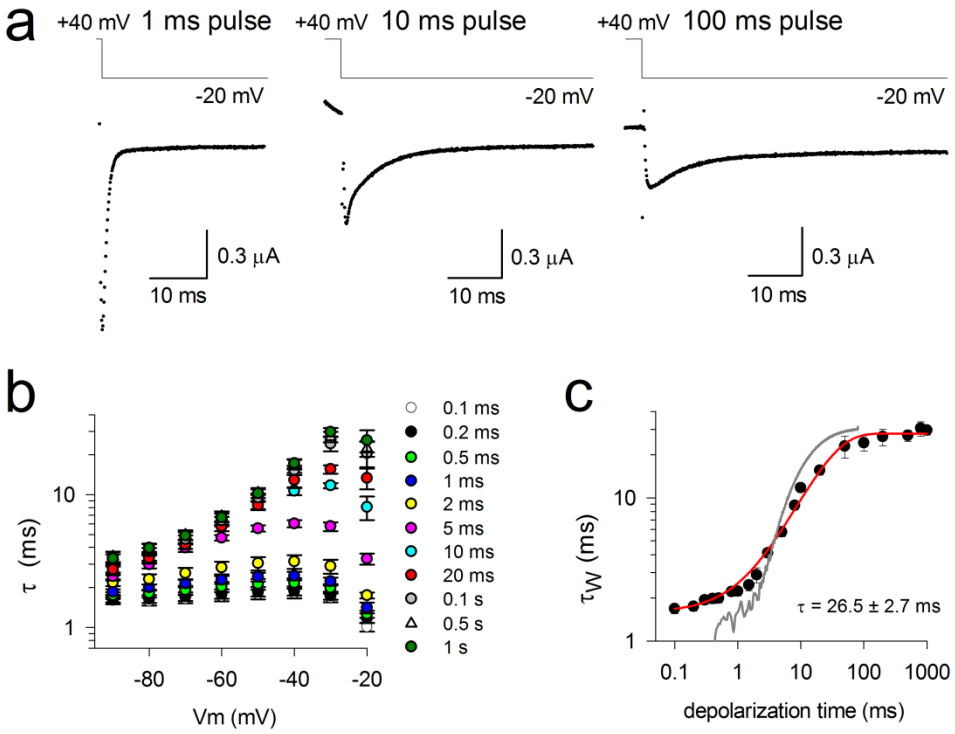

Supplementary Figure 6: I_{Gdeac} decay kinetics of the Shaker_S3S4_K_v3.1 W434F chimera upon different depolarization times.

(**a**) $I_G$deac currents of the Shaker_S3S4_K_v3.1 W434F chimera elicited during repolarization to -20 mV upon a 1, 10 and 100ms depolarization to +40 mV (pulse protocol is shown on top). (**b**) Voltage dependence of the weighted I_{Gdeac} time constants ± SEM (*n* = 6) as a function of depolarizing pulse duration. Note the gradual slowing in I_{Gdeac} kinetics when depolarization times became longer. (**c**) The weighted I_{Gdeac} time constant at -30 mV as a function of depolarization time. The superimposed scaled ionic current activation is shown as a grey trace.

Supplementary Table 1: Parameters for 4-State Markov Model.

Rate constants	Black, pink, green trace	Red trace	Blue trace
α_p / z_p	.05 / 3.5	.05 / 3.5	.05 / 3.5
β_p / z_p	.15 / 3.5	.15 / 3.5	.15 / 3.5
α_I / z_I	6 / .4	6 / .4	6 / .4
β_I / z_I	.6 / .4	1.8 / .4	.4 / .4
α_s / z_s	1 / .001	1 / .001	1 / .001
β_s / z_s	.8 / .001	.8 / .001	.8 / .001

Supplementary Discussion

Voltage-dependence of Shaker_S3S4_K_v3.1 gating currents suggests resurgent current is related to the relaxed state

In WT Shaker channels the total gating charge is distributed across several transitions, including transitions between different closed states[2,3]. For a currently undefined reason, the movement of the early gating charge component between different closed states is facilitated in the Shaker_S3S4_K_v3.1 W434F chimera; that is, this component of the gating charge is shifted towards more hyperpolarized potentials, isolating it from the main gating charge component that is associated with the transition to the pre-activated VSD configuration. Although the resurgent ionic currents of the Shaker_S3S4_K_v3.1 chimera were very similar to those of K_v3.1b, the K_v3.1b gating charge movement showed no such isolation of its early gating charge component. Therefore, the resurgent current most likely does not originate from modifications to the kinetics of this early gating charge component; instead, a process occurring at more positive potentials, such as VSD relaxation, should be responsible.

References

1. Wang, Z., Robertson, B., & Fedida, D. Gating currents from a Kv3 subfamily potassium channel: charge movement and modification by BDS-II toxin. *J. Physiol.* **584**, 755-767 (2007).

2. Bezanilla, F., Perozo, E., & Stefani, E. Gating of *Shaker* K^+ channels: II. The components of gating currents and a model of channel activation. *Biophys. J.* **66**, 1011-1021 (1994).

3. Bezanilla, F. & Villalba-Galea, C. A. The gating charge should not be estimated by fitting a two-state model to a Q-V curve. *J. Gen. Physiol.* **142**, 575-578 (2013).